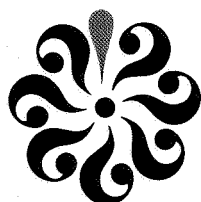


N82-70426

(NASA-CR-164988) CONNECTION BETWEEN WALL
STREAKS AND TIME AVERAGE VELOCITY PROFILES
IN A TURBULENT BOUNDARY LAYER Progress
Report, 4 May - 3 Nov. 1981 (Old Dominion
Univ., Norfolk, Va.) 17 p CSCL 20D 00/34 08297

Unclas
08297

OLD DOMINION UNIVERSITY RESEARCH FOUNDATION



DEPARTMENT OF MECHANICAL ENGINEERING AND MECHANICS
SCHOOL OF ENGINEERING
OLD DOMINION UNIVERSITY
NORFOLK, VIRGINIA

CONNECTION BETWEEN WALL STREAKS AND TIME AVERAGE VELOCITY PROFILES IN A TURBULENT BOUNDARY LAYER

By

Robert L. Ash, Principal Investigator

Progress Report
For the period May 4 - November 3, 1981



Prepared for the
National Aeronautics and Space Administration
Langley Research Center
Hampton, Virginia

Under
Research Grant NAG1-121
Joshua C. Anyiwo, Technical Monitor
High Speed Aerodynamics Division

October 1981

DEPARTMENT OF MECHANICAL ENGINEERING AND MECHANICS
SCHOOL OF ENGINEERING
OLD DOMINION UNIVERSITY
NORFOLK, VIRGINIA

CONNECTION BETWEEN WALL STREAKS AND TIME
AVERAGE VELOCITY PROFILES IN A TURBULENT
BOUNDARY LAYER

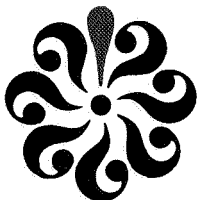
By

Robert L. Ash, Principal Investigator

Progress Report
For the period May 4 - November 3, 1981

Prepared for the
National Aeronautics and Space Administration
Langley Research Center
Hampton, Virginia 23665

Under
Research Grant NAG1-121
Joshua C. Anyiwo, Technical Monitor
High Speed Aerodynamics Division



Submitted by the
Old Dominion University Research Foundation
P.O. Box 6369
Norfolk, Virginia 23508-0369

October 1981

CONNECTION BETWEEN WALL STREAKS AND TIME-AVERAGED VELOCITY
PROFILES IN A TURBULENT BOUNDARY LAYER

By

R. L. Ash*

Abstract

The effect of coherent flow structures on the mean velocity profile of a flat plate boundary layer has been investigated. By assuming the near wall "streak structure" can be modeled by power series expansions in terms of the wall normal coordinate, the equations of motion have been used to define a solution domain. Requirements imposed by the time-averaged wall streak functions can be accommodated by series representations of the mean velocity profile out to y^+ of about 15, where the solution and series begin to depart. That result is in good agreement with the experimental observations of Kline et al.² In addition, the Reynolds stress distribution implied by interpreting the coefficients for the mean velocity profile in terms of streak functions is in good agreement with other data.

*Professor, Department of Mechanical Engineering and Mechanics, Old Dominion University, Norfolk, VA 23508.

Discussion

Recently Cantwell¹ has summarized research on organized structure in turbulent flows. The structural features in a turbulent boundary layer include low-speed streaks near the wall which are intermittent and highly three-dimensional. Kline et al.² in 1967 reported first details of those structures and defined a cycle of events which, though distributed randomly in space and time, are repetitive. If attention is restricted to the simplest case of a constant density, flat plate boundary layer with no pressure gradient, the question of how the three-dimensional, near wall flow structure affects the time-averaged velocity profile can be addressed.

In the vicinity of the wall ($y = 0$), the inner boundary conditions obviously must dominate. Furthermore, it is reasonable to assume that the three-dimensional, unsteady equations of motion have a solution which can be expanded in a power series of y near the wall. The dimensionless governing equations are

$$\vec{\nabla} \cdot \vec{u} = 0 \quad (1)$$

$$\frac{D\vec{u}}{Dt} = -\vec{\nabla}P + \frac{1}{R} \nabla^2 \vec{u} \quad (2)$$

where the velocity vector \vec{u} is made dimensionless with the friction velocity u_τ , the coordinates are normalized with respect to the boundary-layer thickness δ , pressure is normalized with respect to wall shear stress τ_w , and time is expressed in units of δ/u_τ . The term R is a Reynolds number defined by $R = u_\tau \delta / \nu$. It should be noted that the dimensionless

x-component of velocity u , is the same as u^+ , and the dimensionless vertical y-coordinate is related to y^+ by

$$Ry = y^+ \quad (3)$$

If the velocity components u , v , and w , and pressure are assumed expressible in power series of y , consistent with the inner boundary conditions and continuity, they must take the form:

$$u = \sum_{n=1}^{\infty} u_n(x, z, t) y^n \quad (4)$$

$$v = \sum_{n=2}^{\infty} v_n(x, z, t) y^n \quad (5)$$

$$w = \sum_{n=1}^{\infty} w_n(x, z, t) y^n \quad (6)$$

and

$$P = P_w(x, z, t) + \sum_{n=1}^{\infty} P_n(x, z, t) y^n \quad (7)$$

where $P_w(x, z, t)$ is the wall pressure. By equating coefficients with the same powers of y in Eqs. (1) and (2), the terms in the velocity and pressure power series can be related to u_1 , w_1 , and P_w . Consequently,

$$u = u_1 y + \frac{R}{2} \frac{\partial P_w}{\partial x} y^2 + \frac{1}{6} \left[R \frac{\partial u_1}{\partial t} - 2 \frac{\partial^2 u_1}{\partial x^2} - \frac{\partial}{\partial z} \left(\frac{\partial w_1}{\partial x} + \frac{\partial u_1}{\partial z} \right) \right] y^3 \quad (8) \text{ cont'd}$$

$$\begin{aligned}
& + \frac{R}{24} \left\{ \frac{\partial}{\partial x} \left[R \frac{\partial P_w}{\partial t} - 2 \left(\frac{\partial^2 P_w}{\partial x^2} + \frac{\partial^2 P_w}{\partial z^2} \right) \right] + u_1 \frac{\partial u_1}{\partial x} - u_1 \frac{\partial w_1}{\partial z} \right. \\
& \left. + 2w_1 \frac{\partial u_1}{\partial z} \right\} y^4 + \dots
\end{aligned} \tag{8}$$

concl'd

$$\begin{aligned}
v = & -\frac{1}{2} \left(\frac{\partial u_1}{\partial x} + \frac{\partial w_1}{\partial z} \right) y^2 - \frac{R}{6} \left(\frac{\partial^2 P_w}{\partial x^2} + \frac{\partial^2 P_w}{\partial z^2} \right) y^3 + \frac{1}{24} \left[2 \frac{\partial^3 u_1}{\partial x^3} + 2 \frac{\partial^3 w_1}{\partial z^3} \right. \\
& \left. + 2 \frac{\partial^2}{\partial x \partial z} \left(\frac{\partial w_1}{\partial x} + \frac{\partial u_1}{\partial z} \right) - R \frac{\partial}{\partial t} \left(\frac{\partial w_1}{\partial z} + \frac{\partial u_1}{\partial x} \right) \right] y^4 + \dots
\end{aligned} \tag{9}$$

$$\begin{aligned}
w = & w_1 y + \frac{R}{2} \frac{\partial P_w}{\partial z} y^2 + \frac{1}{6} \left[R \frac{\partial w_1}{\partial t} - 2 \frac{\partial^2 w_1}{\partial z^2} - \frac{\partial}{\partial x} \left(\frac{\partial w_1}{\partial x} + \frac{\partial u_1}{\partial z} \right) \right] y^3 + \\
& + \frac{R}{24} \left\{ \frac{\partial}{\partial z} \left[R \frac{\partial P_w}{\partial t} - 2 \left(\frac{\partial^2 P_w}{\partial x^2} + \frac{\partial^2 P_w}{\partial z^2} \right) \right] + w_1 \frac{\partial w_1}{\partial z} - w_1 \frac{\partial u_1}{\partial x} \right. \\
& \left. + 2u_1 \frac{\partial w_1}{\partial x} \right\} y^4 + \dots
\end{aligned} \tag{10}$$

$$\begin{aligned}
P = & P_w - \frac{1}{R} \left(\frac{\partial u_1}{\partial x} + \frac{\partial w_1}{\partial z} \right) y - \frac{1}{2} \left(\frac{\partial^2 P_w}{\partial x^2} + \frac{\partial^2 P_w}{\partial z^2} \right) y^2 + \frac{1}{6R} \left[\frac{\partial^3 u_1}{\partial x^3} + \frac{\partial^3 w_1}{\partial z^3} \right. \\
& \left. + \frac{\partial^2}{\partial x \partial z} \left(\frac{\partial u_1}{\partial z} + \frac{\partial w_1}{\partial x} \right) \right] y^3 + \dots
\end{aligned} \tag{11}$$

These series expansions should represent fully the portion of the three-dimensional flow structure which is dominated by the wall boundary conditions. However, the functional forms of u_1 , w_1 , and P_w cannot be determined without imposing "outer" boundary conditions characterized by the flow structure in the outer portion of the boundary layer. Since "bursting" and "inrush" flow phases are both intermittent and occur at the top of streak structures, application of realistic outer boundary conditions to the streak structures is not currently possible.

Alternatively, if one assumes that the near wall flow structure is represented by Eqs. (8) through (11), the connection between these observed three-dimensional flows and the known two-dimensional time-averaged velocity profiles can be addressed. Kline et al.² found that wall bound "low-speed streaks" were stable out to between 8 and 12 wall units ($8 < y^+ < 12$). They observed further that oscillation and "bursting" of these structures took place when they extended out to between 10 and 30 wall units. Based on those observations, the time-averaged forms of Eqs. (8) through (11) should be consistent with the time-averaged velocity profile data beyond $y^+ = 8$, but not beyond $y^+ = 30$. The x-component of velocity (u) for turbulent flow over a flat plate with no pressure gradient is the most documented experimentally and therefore attention is restricted here to Eq. (8).

Making use of the identity:

$$u_1 \frac{\partial u_1}{\partial x} - u_1 \frac{\partial w_1}{\partial z} + 2w_1 \frac{\partial u_1}{\partial z} = 2 \left(\frac{\partial u_1^2}{\partial x} + \frac{\partial u_1 w_1}{\partial z} + 3u_1 v_2 \right) \quad (12)$$

Eq. (8) can be averaged with respect to time for two-dimensional flow past a flat plate to yield:

$$\bar{u}(y) = \bar{u}_1(x)y - \frac{1}{3} \frac{d^2 \bar{u}_1}{dx^2} y^3 + \left(\frac{R}{12} \frac{d\bar{u}_1^2}{dx} + \frac{R}{4} \overline{u_1 v_2} \right) y^4 + \dots \quad (13)$$

Furthermore, the time average of $u_1(x, z, t)$ must be equal to R .

Now Reynolds number, R , was assumed constant in the dimensionless formulation of the equations of motion. However, in order to investigate the magnitude of the coefficients in Eq. (13), variation of R with dimensionless x must be examined. Schlichting³ has tabulated R , Re_L , and C'_f where Re_L and C'_f are the length-based Reynolds number $\left(\frac{U_\infty L}{\nu} \right)$ and local skin friction coefficient, respectively, over a range of length-based Reynolds numbers from 10^5 to 10^9 . It can be shown that

$$x = \frac{Re_L}{R} \left(\frac{C'_f}{2} \right)^{1/2} \quad (14)$$

and the variation of R with x over the entire range of length Reynolds numbers is shown in Figure 1. For length Reynolds numbers above 200,000, R varies semilogarithmically with x and is well approximated by:

$$R = 2.42 \exp(0.1615 x) \quad (15)$$

Consequently,

$$\frac{d^2 \bar{u}_1}{dx^2} = \frac{d^2 R}{dx^2} \approx 0.026 R \quad (16)$$

For boundary-layer flow, the dimensionless Reynolds stress, $\sigma (= -\overline{uv})$, varies with the third power of y , leaving the wall.⁴ Furthermore, $\overline{u_1 v_2}$ can be related directly to the third derivative of the dimensionless Reynolds stress with respect to y^+ at the wall (σ_w''') by:

$$\frac{R}{4} \overline{u_1 v_2} y^4 = -\frac{1}{24} \sigma_w''' (y^+)^4 \quad (17)$$

and although $\frac{\partial \overline{u_1^2}}{\partial x}$ need not be zero, it must certainly be small compared to $\overline{u_1 v_2}$. Consequently, the coefficient for y^4 in Eq. (13) is well approximated by Eq. (17) and utilizing the fact that $\bar{u} = u^+$, along with Eq. (16), we can write

$$u^+ = y^+ - \frac{8.7 \times 10^{-3}}{R^2} (y^+)^3 - \frac{\sigma_w'''}{24} (y^+)^4 + \dots \quad (18)$$

For y^+ greater than 5, but less than 35, experimental velocity data cannot be approximated simply by either a linear or a logarithmic velocity profile. However, Spalding⁵ and Kleinstein⁶ have shown that experimental velocity profile data in that range are represented very well by the equation

$$y^+ = u^+ + e^{-\kappa B} \left[e^{\kappa u^+} - 1 - \kappa u^+ - \frac{(\kappa u^+)^2}{2} - \frac{(\kappa u^+)^3}{6} \right] \quad (19)$$

where Spalding used $\kappa = 0.4$, $B = 5.5$. That equation cannot be inverted directly to a power series in $u^+(y^+)$, but a polynomial fit of Eq. (19)

is less sensitive to scatter than a polynomial fit of tabulated experimental data.

A regression analysis computer program has been used to generate polynomials in the form

$$u^+ = a_1 y^+ + \sum_{n=3}^{10} a_n \cdot (y^+)^n \quad (20)$$

which approximate Eq. (19) over a prescribed interval $0 < y^+ < y_M^+$, where y_M^+ was varied between 5 and 100. The polynomials were generated by creating data tables consisting of 101 "data points" which were produced by using Eq. (19) to determine a maximum u^+ corresponding to y_M^+ , then computing a set of $y_n^+(u_n^+)$ where $u_n^+ = (n-1)u_M^+/100$. The zero intercept (a_0) and a_2 coefficients were excluded on physical grounds, while a_1 was allowed to vary even though its value was required physically to be unity. The polynomial was truncated at the tenth power because that was considered a high enough power of y^+ to simultaneously allow the regression analysis program to exclude unneeded terms and still remain efficient computationally.

In order to desensitize the polynomial fit from the magnitude of y_M^+ [since $(y_M^+)^{10}$ could be very large], y^+ was normalized in terms of y_M^+ ($\hat{y} = y^+/y_M^+$) and the polynomials were found to take the form

$$u^+ = y_M^+ (b_1 \hat{y} + b_3 \hat{y}^3 - b_4 \hat{y}^4 + b_6 \hat{y}^6 + b_{10} \hat{y}^{10}) \quad (21)$$

over the range $5 < y_M^+ < 20$. Variation of those coefficients with respect to y_M^+ are shown in Figure 2.

Based on previous discussion, b_1 must be unity and, as can be seen in Figure 2, it meets that condition to a very good approximation over the entire range. The constraints imposed on b_3 from Eq. (18) are not as easily met. In fact, since R must be greater than 200 for any turbulent flow, it is apparent from Eq. (18) that b_3 must be a very small negative number. That requirement restricts the polynomial fit to $15 < y_M^+ < 15.3$.

Since $b_3 \approx 0$ for virtually all turbulent boundary-layer flows, that case is taken as the nominally correct polynomial for u^+ in the wall flow regime. There

$$u^+ = 1.00y^+ - 2.21 \times 10^{-4}(y^+)^4 + 7.21 \times 10^{-7}(y^+)^6 - 2.7 \times 10^{-12}(y^+)^{10} \quad (22)$$

The variation of u^+ with y^+ given by Eq. (22) is compared with Eq. (19) using Spaldings' constants in Figure 3. The Figure shows that the curves are essentially identical over the range of the fit and that the polynomial departs rapidly outside of the domain. The good agreement out to a y^+ of about 15 is remarkably consistent with the streak observations of Kline et al.² The present results suggest that three-dimensional flow structures dominated by wall requirements can be modeled out to a y^+ of about 15 where coupled interactions or instabilities must then be considered.

Finally, the fact that b_4 is related directly to the third derivative of $-\overline{uv}$ at the wall can be used as a further check of the physical consistency of Eq. (22). By integrating σ_w''' implied from Eq. (22) and requiring that σ_w, σ_w' and σ_w'' be zero at the wall, it is found that

$$\sigma(y^+) = -\overline{uv}(y^+) = 0.00088 (y^+)^3 + \dots \quad (23)$$

This relationship is compared with Townsend's formula⁷:

$$-\overline{uv} \approx 0.0006 (y^+)^3 \quad (24)$$

and the experimental data of Schubauer⁸ and Laufer⁹ (for a pipe flow) in Figure 4. Since the next term in Eq. (23) will necessarily reduce the magnitude of $-\overline{uv}$, the agreement of the present analysis with the other data is very good.

Conclusions

We have shown that a polynomial fit of Spaldings' equation⁵ for u^+ yields a solution which is consistent with requirements imposed by a time-averaged solution to the equations of motion. If one accepts the hypothesis that the flow structures along the wall of a flat plate, turbulent boundary layer should be modeled mathematically as power series in y , the time average of that solution is consistent with classical velocity profile data out to $y^+ = 15$. At that point, the coefficients in the polynomial fit begin to diverge from the requirements imposed by the equations of motion. These results are consistent with the streak observations of Kline et al.², and our results suggest that the mathematical character of the streak structure changes above y^+ of 15.

A logical explanation for that change is intermittent coupling between outer and inner flow structures beyond $y^+ = 15$. Coupling may either be through a superposition of two structures or an instability produced by a disturbance from the outer flow. Under those conditions, the wall-

controlled solution is applicable for only part of the cycle. Concurrently, the results suggest that a series solution which is in some sense periodic in z and t can be employed to model streaks out to y^+ of 15 without direct consideration of the outer flow structures.

Finally, the good agreement between the Reynolds stress estimation resulting from this approach and experimental data suggests that the polynomial series based on a wall flow structural hypothesis is consistent with the observed physics.

References

- ¹ B.V. Cantwell, in Annual Review of Fluid Mechanics, Edited by M.D. Van Dyke, J.V. Wehausen and J.L. Lumley, 13, 457 (1981).
- ² S.J. Kline, W.C. Reynolds, F.A. Schraub and P.W. Runstadler, J. Fluid Mech., 30, 741 (1967).
- ³ H. Schlichting, Boundary Layer Theory, 6th Ed., McGraw Hill, New York, (1968), p. 603.
- ⁴ Hinze, J.O., Turbulence, 2nd Edition, McGraw-Hill, New York (1975), p. 620.
- ⁵ D.B. Spalding, J. Applied Mech., 28, 455 (1961).
- ⁶ G. Kleinstein, AIAA J., 5, 1402 (1967).
- ⁷ A.A. Townsend, The Structure of Turbulent Shear Flow, Cambridge University Press (1956), p. 227.
- ⁸ G. B. Schubauer, J. Applied Phys., 25, 188 (1954).
- ⁹ J. Laufer, The Structure of Turbulence in Fully Developed Pipe Flow. N.A.C.A. Rep. No. 1174 (1954).

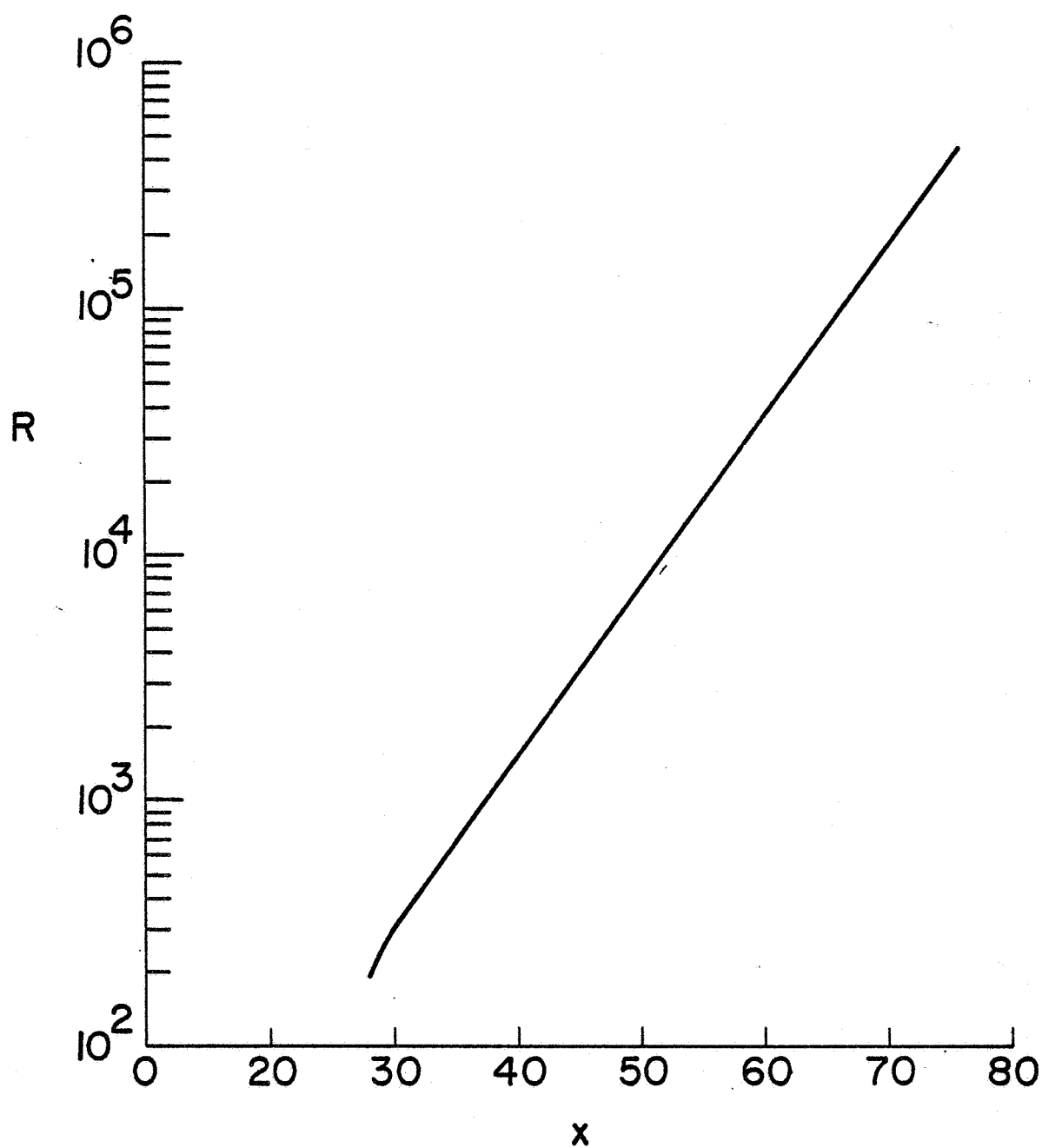


Figure 1. Variation of Reynolds number (R) with downstream distance in units of boundary-layer thickness.

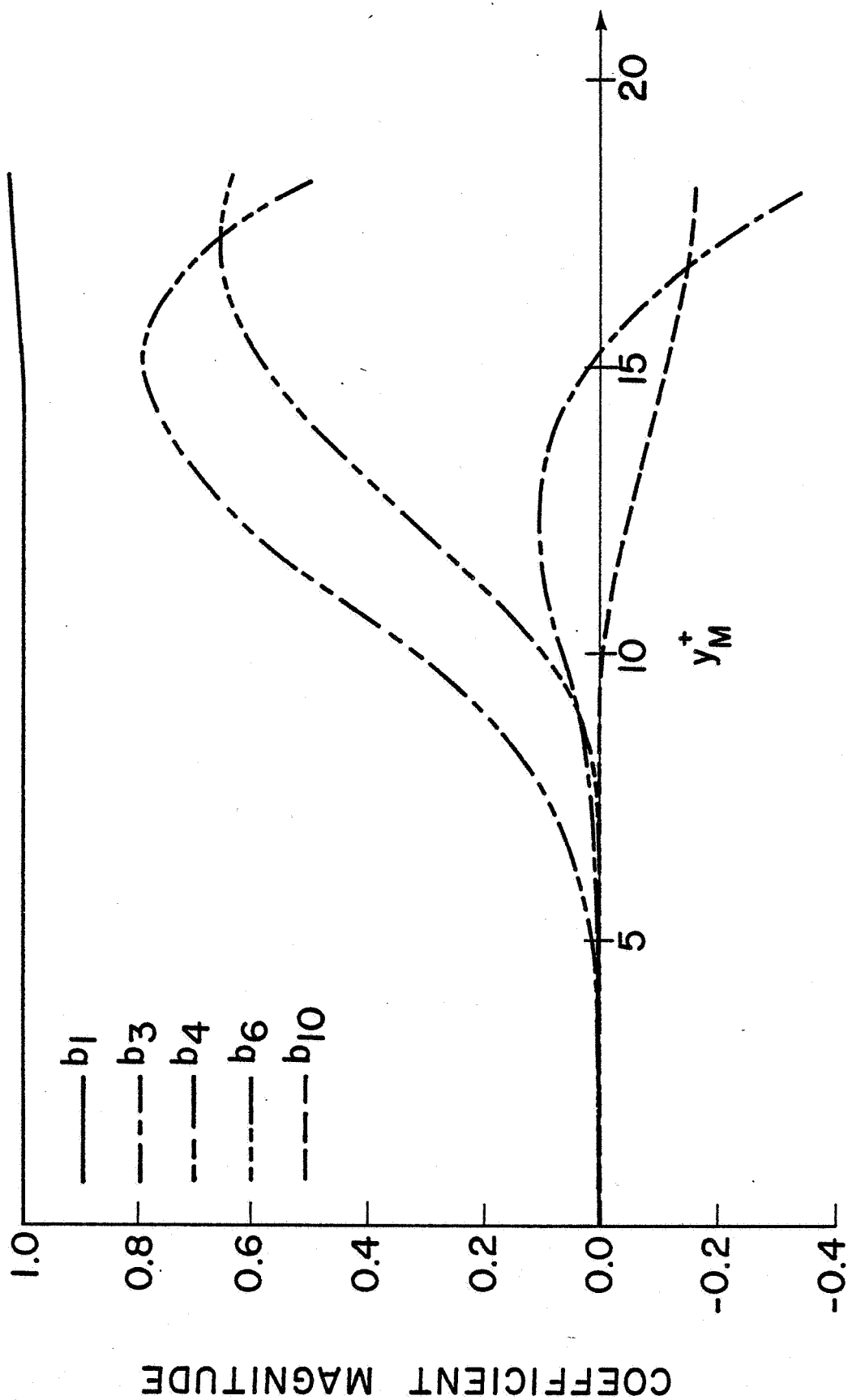


Figure 2. Variation of the coefficients in Eq. (21) with y_M^+ .

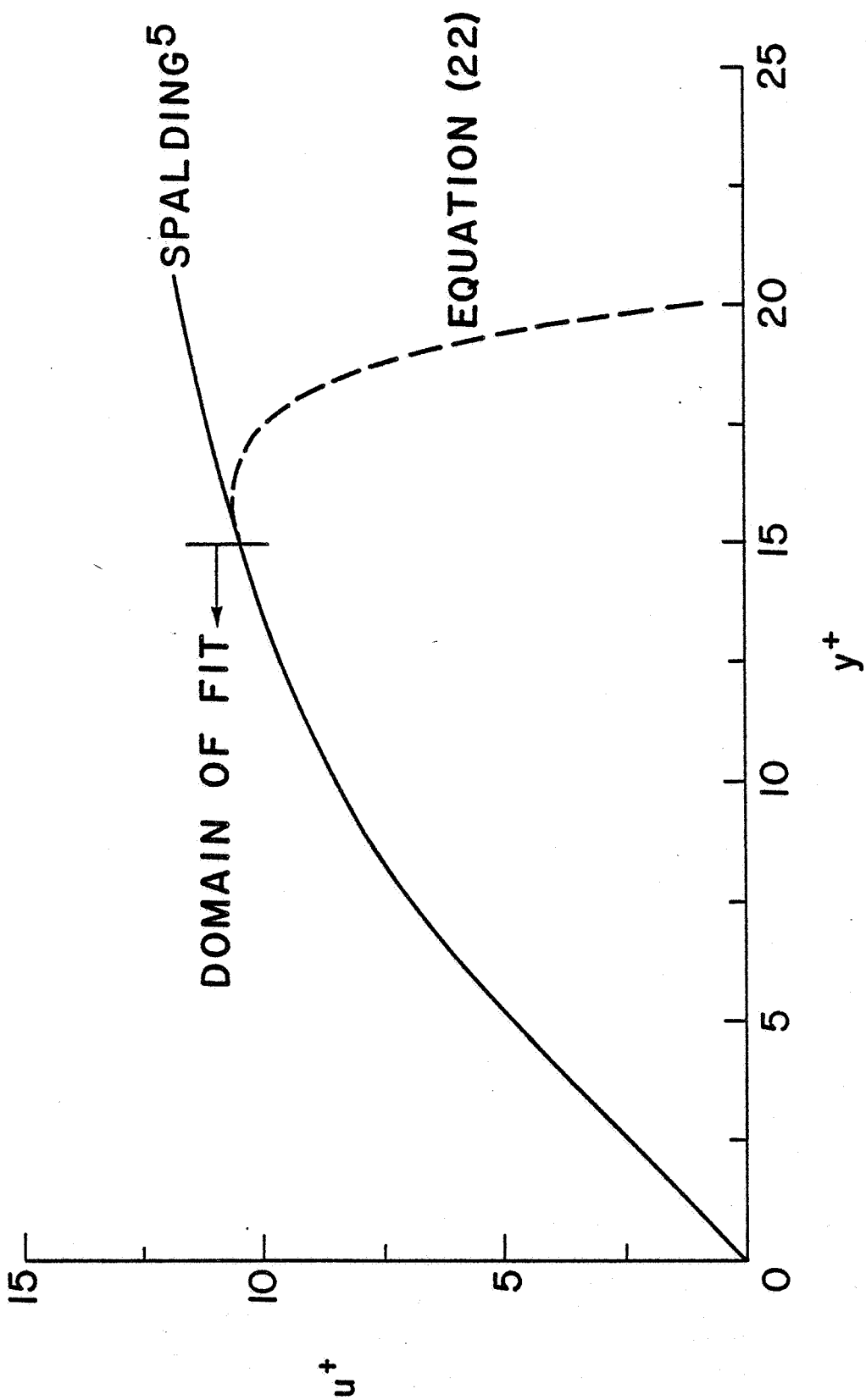


Figure 3. Comparison between the velocity profile from Eq. (19) with the regression fit of Eq. (22).

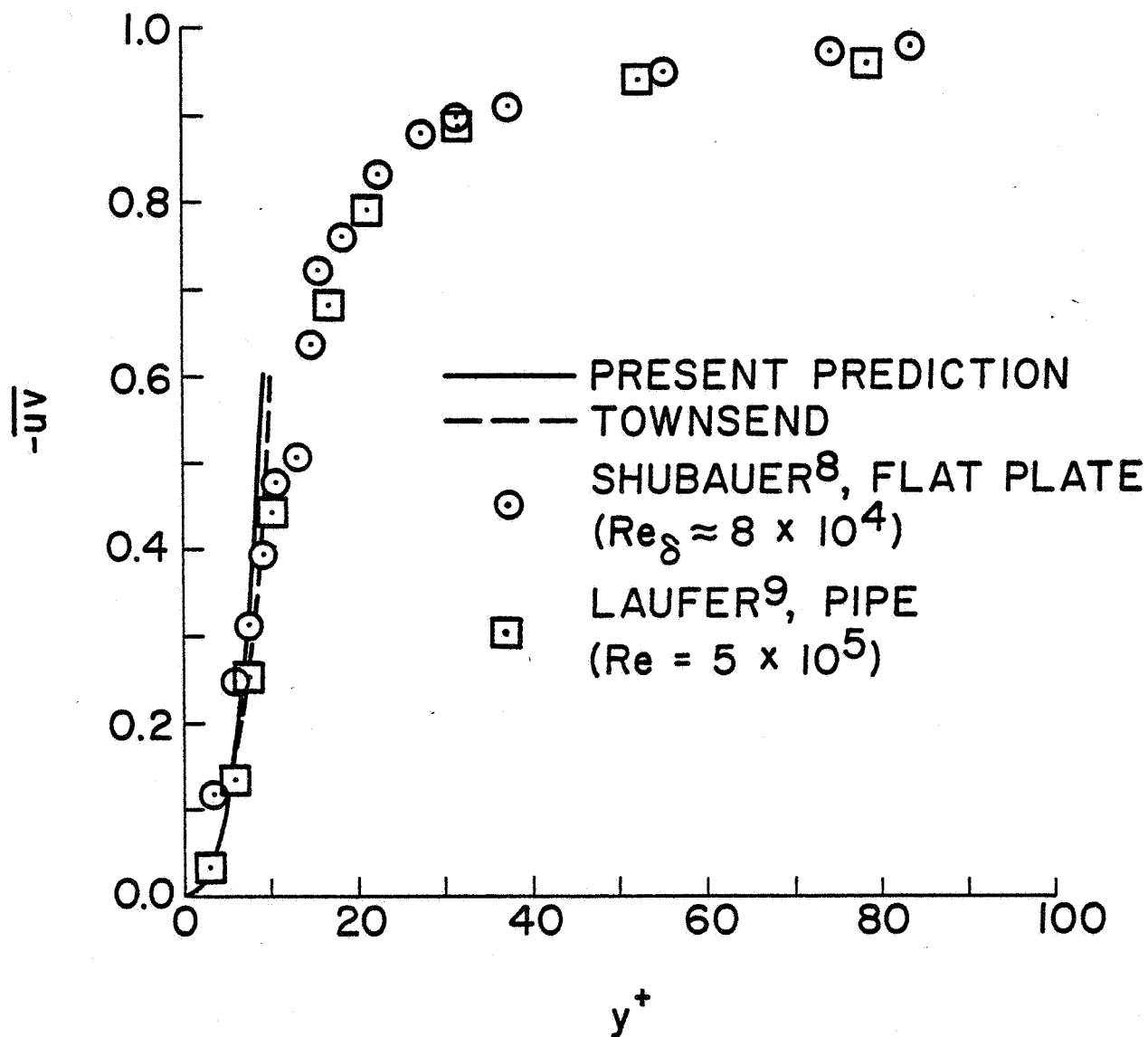


Figure 4. Comparison between the predicted Reynolds stress leaving the wall and the experimental measurements of Schubauer⁸ and Laufer⁹.